Pergamon

Int. J. Solids Structures Vol. 32, No. 23, pp. 3407–3421, 1995

0020–7683/95 $9.50 + .00

0020–7683(94)00314–9

RESPONSE OF AN ELASTIC, PLASTIC TUBULAR CANTILEVER BEAM SUBJECTED TO A FORCE PULSE AT ITS TIP—SMALL DEFLECTION ANALYSIS

S. R. REID, T. X. YU and J. L. YANG
Department of Mechanical Engineering, UMIST, P.O. Box 88, Manchester, U.K.

(*Received* 7 *July* 1994; *in revised form* 20 *November* 1994)

Abstract—According to experiments, the bending behaviour of a pipe is characterized by its global elastic–plastic(hardening–softening) bending moment–curvature constitutive equation which depends on the interaction between its material properties and the ovalization of the cross-section when it is subjected to large plastic deformation. In the context of dynamic structural plasticity, this behaviour should have an important role in problems such as pipe-whip. This paper presents the results of a study of the dynamic response of a tubular cantilever beam which possesses such hardening–softening behaviour in the plastic range. With the help of a numerical approach based on a small deflection formulation, three examples are given. The first example which utilizes parameters selected from a typical pipe-whip test is compared with experimental data and gives a good prediction of the degree of ovalization of the cross-section, the distribution of plastic work in the pipe and the instantaneous deformation of the pipe. Additional examples consider various pulse loadings and constitutive relations to demonstrate that the evolution of softening can undergo three stages, viz. initial softening of one cross-section, growth of the softening region and finally shrinking of the softening region to a particular cross-section which exhibits a sharp localization of the bending deformation.

NOTATION

D	diameter of a tubular beam
E	Young's modulus
f_e, f_h, f_s	positive functions
I	second moment of area of the tubular cross-section about the neutral axis
J	rotary inertia of a cross-section per unit length of the tubular beam
L	length of the tubular beam
M	bending moment
M_e	maximum elastic bending moment
M_0	fully plastic bending moment
m	mass per unit length of a tubular beam
$P(t)$	concentrated force pulse
$p(x, t)$	distributed load along a tubular beam
Q	shear force
t	time
w	transverse displacement
x, y	coordinates
κ	curvature
κ_{cr}	critical curvature
κ_d	curvature at the instant unloading occurs
κ_e	elastic limit curvature
κ_g	reversed yielding curvature
α	coefficient defined in Example 3
$\dot{(\ )}$	$\partial(\ )/\partial(t)$
Δ	increment

1. INTRODUCTION

The authors and their co-workers have, over the past 5 years, completed a systematic experimental and theoretical programme of research on the dynamic plastic behaviour of tubular beams in relation to the problem of pipe-whip (Reid and Prinja, 1989; Wang, 1991). This work has demonstrated that a relatively simple rigid, perfectly-plastic beam

model gives reasonable agreement with experimental observations of the response of a pipe to the blow-down force produced when pipe rupture is simulated (Wang, 1991).

The discrepancies between the theoretical predictions and experimental observations were mainly attributed to the effects of hardening and softening in the plastically deformed tubular beams. However in reality, the plastic behaviour of tubular beams is significantly different from that of a beam with a solid section. Hardening and softening resulting from the influence of the material properties and the ovalization of the beam cross-sections greatly affect the dynamic plastic behaviour of tubular beams. In particular the rigid-plastic approach or even a conventional elastic–plastic analysis is unable to represent the local deformation of a tubular beam under intense dynamic loading. In order to study the effects of hardening/softening on the dynamic response of pipes under pulse or impulsive loading, a new study, the preliminary results of which are given herein, has been made of the problem based upon a more general constitutive model for the beam (pipe).

The behaviour of a pipe under a quasi-static bending moment, has received a lot of attention since the initial work of Brazier (1926) who studied the ovalization of a pipe under pure bending in the elastic range. Several studies [e.g. Reddy (1979); Kyriakides and Ju (1992)] have extended this work into the plastic regime for quasi-static loading but the dynamic plastic behaviour of a tubular beam with such hardening/softening properties under intense dynamic loading has not been studied extensively. There are a few publications [e.g. Jones and Wierzbicki (1987); Stronge and Yu (1989); Martin (1989)] which do explore failure mechanisms in relation to pipe-whip problems and other structures in which softening effects occur, such as those resulting from material damage mechanisms, e.g. micro-cracks. The dynamic response of a strain-softening (or hardening) cantilever beam subjected to impulsive loading was considered by Stronge and Yu (1989) who assumed that the cantilever possesses a rigid, plastic, linear-softening (or hardening) moment–curvature characteristic. However they ignored the inertia forces in the plastically deforming segment in the initial, transient stage of the deformation. It was made clear by Stronge and Yu (1989) that this model does not give a realistic representation of the transient stage of deformation of either a strain-hardening or strain-softening cantilever because it neglects elastic effects. Nevertheless, the study is of interest here because it again demonstrates that elastic effects can significantly influence the dynamic plastic behaviour of a structure, especially, when the aim is to predict local deformation and study failure criteria under intense dynamic loading. This issue was examined carefully for solid section cantilever beams by Reid and Gui (1987) who demonstrated the significant role of elasticity in the final distribution of plastic deformation in an elastic, perfectly-plastic beam of solid cross-section.

In connection with failure criteria, Jones and Wierzbicki (1987) discussed some forms of local failure of thin-walled beams, and suggested that the failure mode could be represented by a softening moment–rotation characteristic for the beam as shown in Fig. 1 but no detailed analysis was given. The work of Martin (1989), who examined the failure mode of a cantilever beam subjected to impact may be regarded as an extension of the discussion given by Jones and Wierzbicki (1987). He used a rectangular shape for the

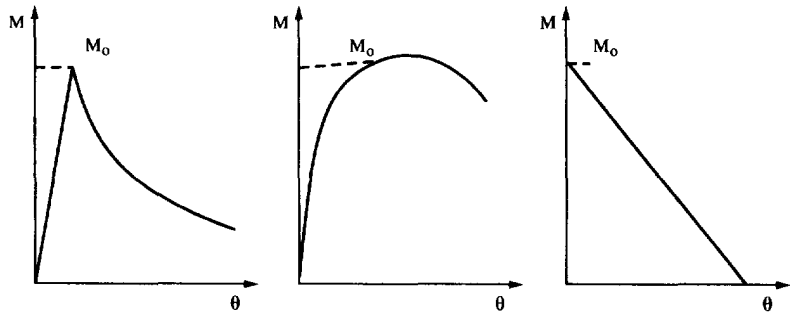

Fig. 1. Typical moment–rotation characteristics: (a) elastic-brittle beam or elastically buckled long cylinder; (b) plastically deforming thicker tube; (c) simple rigid-softening computational model.

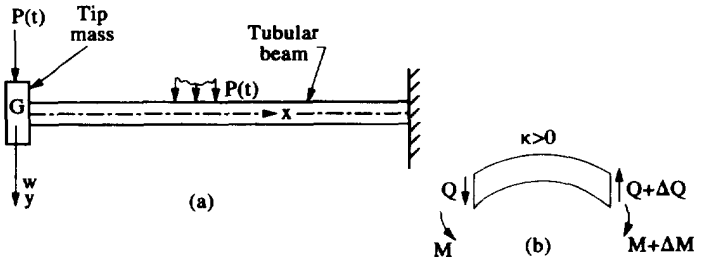

Fig. 2. (a) Elastic, plastic tubular cantilever beam; (b) beam element in deformed configuration.

relationship between the moment and angle of rotation at a plastic hinge to describe the softening behaviour of the beam. His theory is also based on the assumption of rigid, plastic material behaviour. The softening region was found not to expand and the localized deformation took place at a single plastic hinge in the beam.

The aim of this study is to analyse the dynamic behaviour of an elastic, plastic tubular cantilever beam subjected to pulse-loading. In the plastic range, the tubular beam displays hardening and softening behaviour, i.e. its moment–curvature characteristic has a monotonically increasing portion followed by a monotonically decreasing portion in which the effects of ovalization dominate over the material hardening effects. Numerical solutions based on a small deflection formulation with parameters selected from a previously performed pipe-whip test are given and compared with the experimental data for the initial stages of the deformation. Further features of the influence of hardening and softening characteristics are illustrated by means of two further examples.

2. ANALYSIS

2.1. *Equations of motion*

Figure 2(a) shows a tubular cantilever beam of length L carrying an end mass and loaded by a force pulse at its tip. Its behaviour is characterized by its global elastic, plastic (hardening/softening) properties due to the strain-hardening of the material and the ovalization of the tubular cross-section when it is subjected to a bending moment, as indicated in Fig. 3. Suppose that the diameter D of the tubular beam is much smaller than its length L, so that the effects of shear can be neglected. However, the rotary inertia of the tubular cross-section will be taken into account in order to model more precisely the propagation of the elastic flexural deformation.

A typical deformed element of the tubular beam is as shown in Fig. 2(b), the x and y axes being in the axial and transverse directions of the beam, respectively. The external

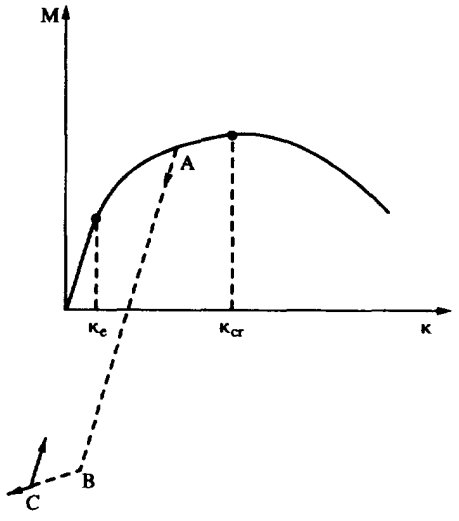

Fig. 3. Constitutive relation for a tubular beam.

force acting on the element, $p(x, t)$, is in the transverse direction only and the deflection is assumed to remain small. Thus the internal generalized forces acting on the element are the shear force Q and the bending moment M. The equations of motion of the element are

$$\frac{\partial Q}{\partial x} + m\ddot{w} = p(x, t) \tag{1}$$

$$\frac{\partial M}{\partial x} - Q = J\frac{\partial \ddot{w}}{\partial x}, \tag{2}$$

where w is the deflection in the y direction and, m and J are the mass and rotary inertia per unit length of the beam. Eliminating the shear force, Q, between these equations leads to

$$\frac{\partial^2 M}{\partial x^2} + m\ddot{w} - J\frac{\partial^2 \ddot{w}}{\partial x^2} = p(x, t). \tag{3}$$

Equation (3) is applicable to beams made of arbitrary material.

2.2. *Constitutive relations*

The general constitutive relation between the bending moment and curvature for a typical tubular beam which possesses elastic and hardening and softening plastic behaviour can be written in the form (see Fig. 3):

$$M = \begin{cases} f_e(\kappa) & 0 \leqslant \kappa \leqslant \kappa_e \\ f_h(\kappa) & \kappa_e < \kappa \leqslant \kappa_{cr}\,;\, \Delta\kappa \geqslant 0 \\ f_s(\kappa) & \kappa_{cr} < \kappa\,;\, \Delta\kappa \geqslant 0, \end{cases} \tag{4a}$$

where $\kappa = \partial^2 w/\partial x^2$ for cases of small deflections. κ_e and κ_{cr} are respectively the elastic limit curvature and the critical curvature at which the transition from a hardening state into a softening state occurs. $f_e(\kappa)$, $f_h(\kappa)$ and $f_s(\kappa)$ are positive functions which describe the characteristics of the deformed tube in the elastic phase, the hardening plastic phase and the softening plastic phase, respectively, and $\Delta\kappa$ is the increment in curvature over a time interval Δt.

Equation (4a) is valid only for loading states ($\Delta\kappa > 0$) in the plastic range. If $\Delta\kappa < 0$ after $\kappa > \kappa_e$, elastic unloading or reversed yielding will take place, the M-κ relation follows the curve ABC as shown in Fig. 3 which is based on the assumption that the tubular beam has isotropic behaviour, thus, for $\Delta\kappa < 0$

$$M = \begin{cases} M_d + EI(\kappa - \kappa_d) & \kappa_d - \dfrac{2M_d}{EI} < \kappa < \kappa_d \\ -f_h(\kappa_d + |\kappa - \kappa_g|) & \kappa_d < \kappa_{cr}\,;\, \kappa < \kappa_d - \dfrac{2M_d}{EI} \\ -f_s(\kappa_d + |\kappa - \kappa_g|) & \kappa_d > \kappa_{cr}\,;\, \kappa < \kappa_d - \dfrac{2M_d}{EI}, \end{cases} \tag{4b}$$

where κ_d and M_d are the curvature and bending moment, respectively, of the cross-section at the instant when unloading starts and κ_g is the reversed yielding curvature which is given by

$$\kappa_g = \kappa_d - \frac{2M_d}{EI}. \tag{4c}$$

Generally speaking several loading and unloading cycles may occur at some cross-sections during the dynamic response of the beam. For this situation, similar steps to those described above are followed.

The derivation of the relationship between M and κ for a beam with elastic–hardening/softening plastic behaviour is in itself an interesting topic. However this is beyond the scope of the present paper which employs the results described in a recent paper by Yu *et al.* (1993).

2.3. *Governing equations and discretation*

The equation of motion, eqn (3) together with the constitutive equations (4) constitute a closed set of non-linear partial differential equations with floating boundaries between the various regions, e.g. between the elastic and hardening regions, the hardening and softening regions, and the plastic and unloading regions. It is difficult if not impossible to obtain an analytical solution for this floating boundary value problem in a finite beam. However, the equations can be solved by numerical means, which are capable of predicting the dynamic response of the tubular beam in the early, transient stages. The details of the final shape of the beam in practically important problems (e.g. pipe-whip) require a large deformation analysis which is currently being completed but the present theory brings out the important phenomenon of localization of deformation which stems from the softening characteristics.

Equations (3) and (4) can be rewritten in finite-difference form. If the beam is divided into elements of length Δx_i, then the governing equations for an element at the ith position are

$$J\ddot{w}_{i+1} - [2J + m(\Delta x_i)^2]\ddot{w}_i + J\ddot{w}_{i-1} = M_{i+1} - 2M_i + M_{i-1} - p_i(\Delta x_i)^2, \quad i = 1, \ldots, n \tag{5}$$

where

$$M_i = \begin{cases} f_e(\kappa_i) & \kappa_i \leqslant \kappa_e \\ f_h(\kappa_i) & \kappa_e < \kappa_i \leqslant \kappa_{cr};\ \Delta\kappa_i \geqslant 0 \\ f_s(\kappa_i) & \kappa_{cr} < \kappa_i;\ \Delta\kappa_i \geqslant 0 \end{cases} \tag{6a}$$

during loading, or, for $\Delta\kappa_i < 0$

$$M_i = \begin{cases} M_{di} + EI(\kappa_i - \kappa_{di}) & \kappa_{di} - \dfrac{2M_{di}}{EI} < \kappa_i < \kappa_{di} \\ -f_h(\kappa_{di} + |\kappa_i - \kappa_{gi}|) & \kappa_{di} < \kappa_{cr};\ \kappa_i < \kappa_{di} - \dfrac{2M_{di}}{EI} \\ -f_s(\kappa_{di} + |\kappa_i - \kappa_{gi}|) & \kappa_{di} > \kappa_{cr};\ \kappa_i < \kappa_{di} - \dfrac{2M_{di}}{EI}, \end{cases} \tag{6b}$$

during unloading and reversed yielding, and

$$\kappa_i = \frac{w_{i+1} - 2w_i + w_{i-1}}{(\Delta x_i)^2}$$

$$\dot{\kappa}_i = \frac{\dot{w}_{i+1} - 2\dot{w}_i + \dot{w}_{i-1}}{(\Delta x_i)^2}. \tag{7}$$

Solving these equations gives the instantaneous values of accelerations $\ddot{w}_i$ at any instant

t_j, thus for the next instant $t_{j+1} = t_j + \Delta t$, the displacements $w_{i,j+1}[= w_i(t_{j+1})]$ in the finite difference notation is deduced from

$$w_{i,j+1} = \ddot{w}_{i,j}(\Delta t)^2 + 2w_{i,j} - w_{i,j-1}. \tag{8}$$

Accordingly, at the instant t_{j+1}, the curvature $\kappa_{i,j+1}[= \kappa_i(t_{j+1})]$ at the ith position is calculated from eqn (7), and $M_{i,j+1}[= M_i(t_{j+1})]$ is then calculated by making use of eqn (6).

2.4. *Computational procedure*

The computational procedure can be summarized as comprising the following steps when the quantities $w_{i,j}$ and $M_{i,j}$ are known for all the points in the tubular beam at time t_j. (i) Solve the linear algebraic equations (5) to calculate the acceleration $\ddot{w}_{i,j}$ at instant t_j. (ii) Using eqn (8), calculate the displacement $w_{i,j+1}$ at the instant $t_{j+1} = t_j + \Delta t$, where Δt is the time increment. (iii) Using eqns (7) and (6) calculate $\kappa_{i,j+1}$ and $M_{i,j+1}$, the values of κ_i and M_i at the instant t_{j+1}. This cycle of computations continues, step by step, until all of the quantities in the response process at any time have been obtained.

3. NUMERICAL RESULTS AND DISCUSSION

3.1. *Pipe-whip analysis*

All of the parameters selected in this example are based on an actual pipe-whip test, Test 4 (Wang, 1991). The cantilever tubular beam was made of mild steel and had outer diameter $D = 50.8$ mm, wall-thickness $h = 2.6$ mm and length $L = 3$ m. It had a concentrated mass G (a 90° elbow and flanged pressure-release device) at its tip. No external load was applied to the beam except for a concentrated force pulse applied at the tip, which, according to the actual pressure pulse measurements, was as shown in Fig. 4 and can be expressed approximately by

$$P(t) = \begin{cases} 11.25 - 1171.88t & 0 < t \leqslant 0.004 \\ 6.56 & 0.004 < t \leqslant 0.017 \\ 6.56 + 937.5(t - 0.017) & 0.017 < t \leqslant 0.022 \\ 11.25 - 192.3(t - 0.022) & 0.022 < t \leqslant 0.035 \\ 8.75 - 15.63(t - 0.035) & 0.035 < t, \end{cases} \tag{9}$$

where the units for P and t are kilonewtons (kN) and seconds (s), respectively.

The derivation of the constitutive relations (M-κ) of the tubular beam for the hardening and softening phases used in this example is given by Reid *et al.* (1992). It is based on the analysis of ovalization given by Calladine (1982). An initial elastic phase is followed by a hardening portion which is represented by a polynomial in κ. This ensures continuity of

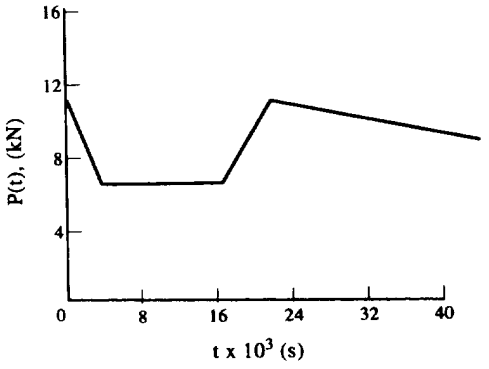

Fig. 4. Shape of pulse load from actual measurements.

Table 1. Data for pipe-whip Test 4

Mass per unit length of the pipe	$m = 3.22$ kg/m
Concentrated tip mass	$G = 1.80$ kg
Second moment of area of the cross-section about the neutral axis	$I = 13.378 \times 10^{-8}$ m^4
Polar moment of inertia of pipe cross section per unit length of the pipe	$J = 1.0387 \times 10^{-3}$ kg/m
Young's modulus	$E = 200$ GN/m^2
Maximum elastic bending moment	$M_e = 1050$ Nm
Fully plastic bending moment	$M_0 = 1750$ Nm
Maximum elastic curvature	$\kappa_e = 0.03924$ m^{-1}
Critical curvature	$\kappa_{cr} = 1.54$ m^{-1}
Length of each element (Number of elements = 60)	$\Delta x = 50$ mm

slope in the M-κ relations at the transition from elastic behaviour and incorporates the critical moment and curvature corresponding to the onset of softening given by Calladine.

(1) Elastic phase

$$M(\kappa) = EI\kappa \quad \text{for} \quad 0 \leqslant \kappa \leqslant \kappa_e$$

(2) Hardening plastic phase

$$M(\kappa) = 1050 + 920\kappa - 300\kappa^2 \quad \text{for} \quad \kappa_e < \kappa \leqslant \kappa_{cr}$$

(3) Softening plastic phase

$$M(\kappa) = 1900(1.0 - 0.031\kappa^2) \quad \text{for} \quad \kappa_{cr} < \kappa.$$

Other parameters used in the example are given in Table 1.

Figure 5 shows the distribution of curvature along the tubular cantilever beam at various instants during the response. The softening phase is initiated at $t \approx 32$ ms and at the position approximately 0.85 m from the tip of the beam. The experimental data (see Fig. 6) indicate that the most ovalized cross-section is at approximately 0.762 m away from the tip. The difference between numerical prediction and experimental measurement is

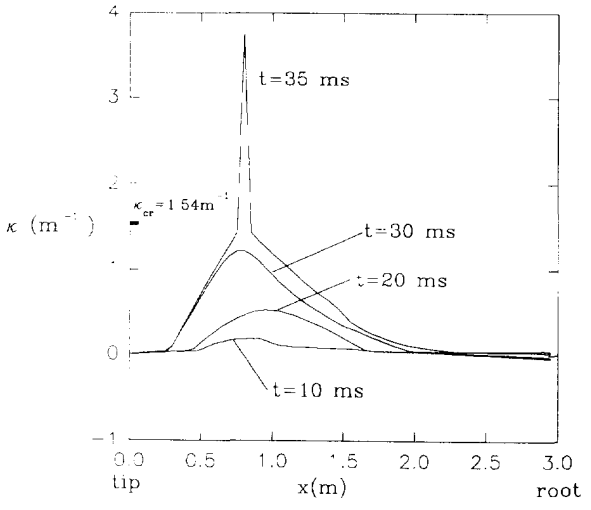

Fig. 5. The distribution of curvature.

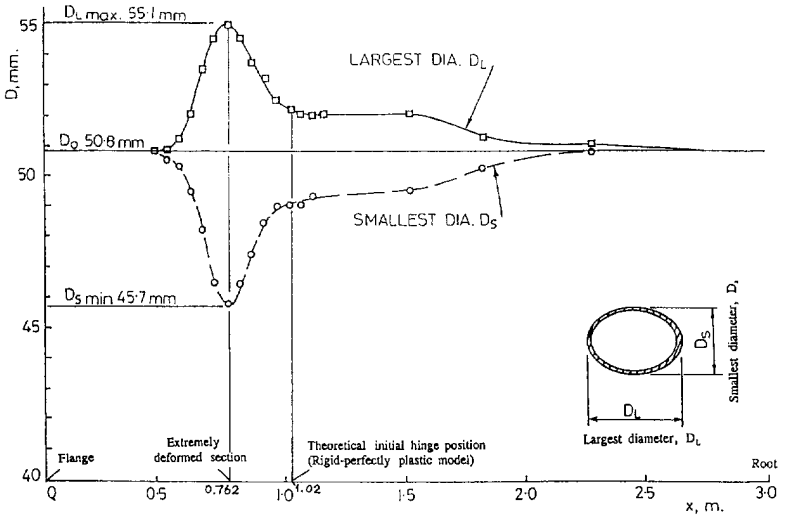

Fig. 6. Variation of the largest and smallest diameters of the deformed pipe along pipe length, measured from a pipe-whip specimen of 2 inch diameter, loaded to 1000 psi (Test 4). x was measured from the pipe tip.

about 10%. It is also evident from Figs. 5 and 6 that the numerical results provide good estimates for the axial distribution of plastic deformation measured after the tests. In this example, when the cross-section which has the maximum curvature in the hardening phase reaches the critical curvature κ_{cr}, the succeeding softening character is restricted to that cross-section only and its curvature increases sharply while the neighbouring sections undergo unloading.

Instantaneous profiles of the centre line of the deformed tubular beam obtained by numerical calculation are as shown Fig. 7. As a comparison, some experimental data obtained from a series of high speed photographs which were taken in Test 4 are also shown in Fig. 7. The profiles agree reasonably well with each other, given the limitations of the small deflection approximation.

Tip deflection, one of the important parameters in the study of pipe-whip, is plotted against time in Fig. 8 where both numerical results and experimental data are included. Again, good agreement is noted.

The instantaneous distributions of bending moment along the deformed tubular beam are plotted in Fig. 9. They confirm the point of view expressed by Symonds and Fleming (1984), and Reid and Gui (1987) that the moment distributions in an elastic–plastic beam

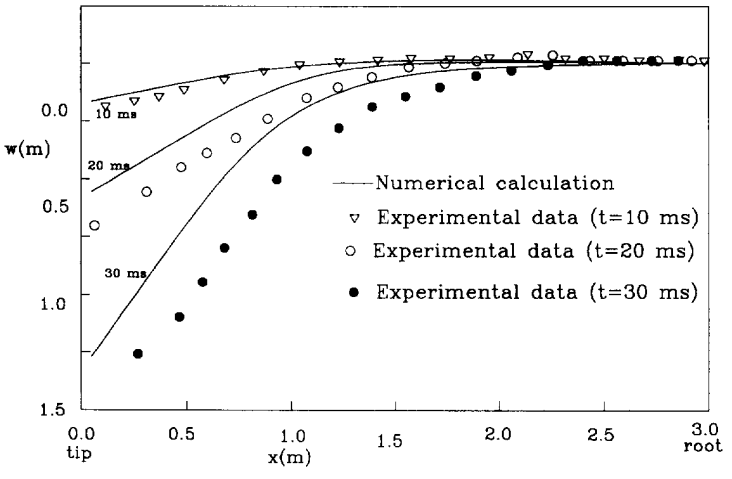

Fig. 7. Deflected shapes of the pipe at various instants.

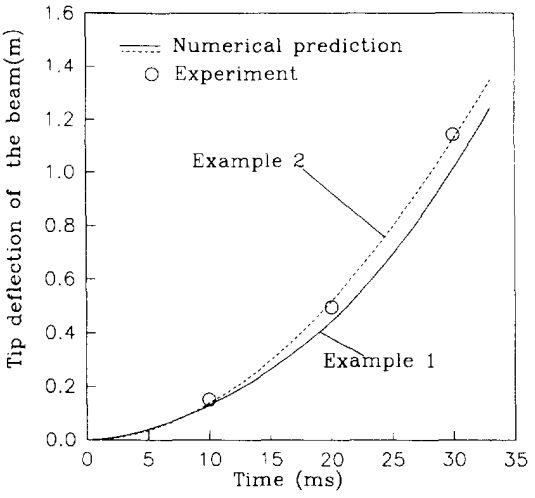

Fig. 8. Tip deflection of the pipe.

differ markedly from those predicted by a rigid-plastic beam analysis in some stages of the deformation. In particular the occurrence of a negative plastic bending moment at the root and the oscillation of the position of the peak moment around the middle part of the beam are both features of the present analysis as they were of the analysis given by Reid and Gui (1987). In the Appendix the present analysis is applied specifically to one of the problems solved by Reid and Gui and close agreement between the two approaches is demonstrated.

3.2. *Rectangular pulse loading*

All of the parameters selected in this example are identical to those in Section 3.1 with the exception that shape of the force pulse applied to the tip is taken to be a step force $\bar{P}$ with magnitude

$$\bar{P} = \int_0^{35(\mathrm{ms})} P(t)\,\mathrm{d}t/35(\mathrm{ms}) = 8442\,(\mathrm{N}),$$

where $P(t)$ is defined in eqn (9). The distributions of curvature and bending moment along

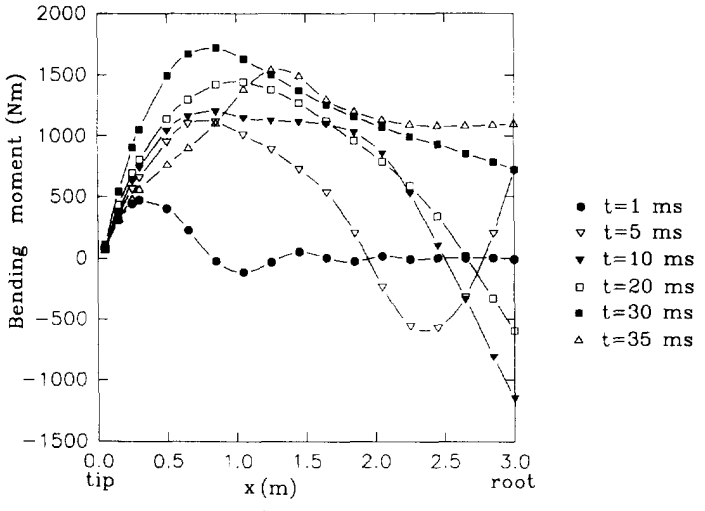

Fig. 9. The distribution of bending moment.

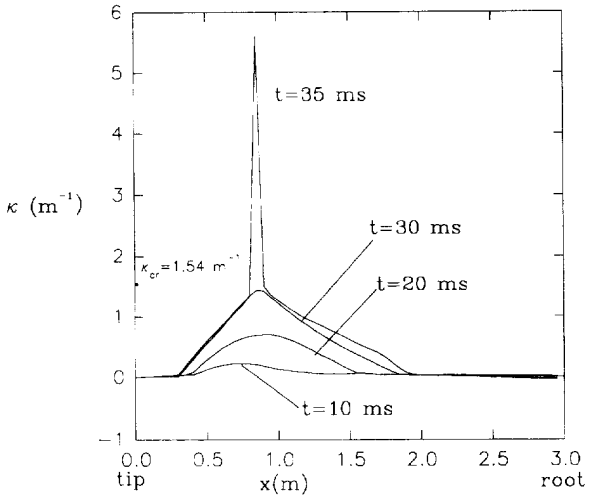

Fig. 10. The distribution of curvature.

the tubular cantilever beam at various instants are shown in Figs 10 and 11, respectively. A notable difference between this case and that described in Section 3.1 is that, in the softening phase, the softening region expands when a rectangular pulse is applied. A neighbouring cross-section which is 50 mm away from the initial softening cross-section enters the softening state. The softening region then shrinks to a single cross-section while the neighbouring cross-sections undergo unloading. This phenomenon is shown in Fig. 12 which give a summary of the evolution of the plastic regions during the response.

The tip deflection against time for Example 2 is plotted in Fig. 8, which actually gives a closer fit to the experimental data than that given by Example 1.

3.3. *Examples of the development of a softening region*

In the previous two sections examples have been given in which the constitutive equation was selected from Reid *et al.* (1992) based on experimental observations. According to these calculations, it seems that the softening region undergoes virtually no growth, the curvature $\kappa(>\kappa_{cr})$ at any time being confined to only one or two cross-sections in the tubular beam. At first this is something of a puzzle when comparing this phenomenon with the results obtained by Yu and Li (1993) and Wang *et al.* (1994) in which the softening region develops with time for semi-infinite beams subjected to a constant velocity at the tip. It should be noted, however, that in the present study the beam is finite and clamped

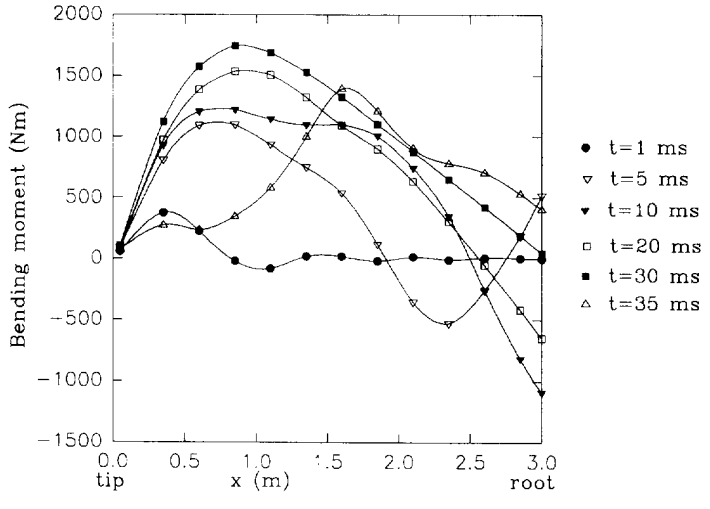

Fig. 11. The distribution of bending moment.

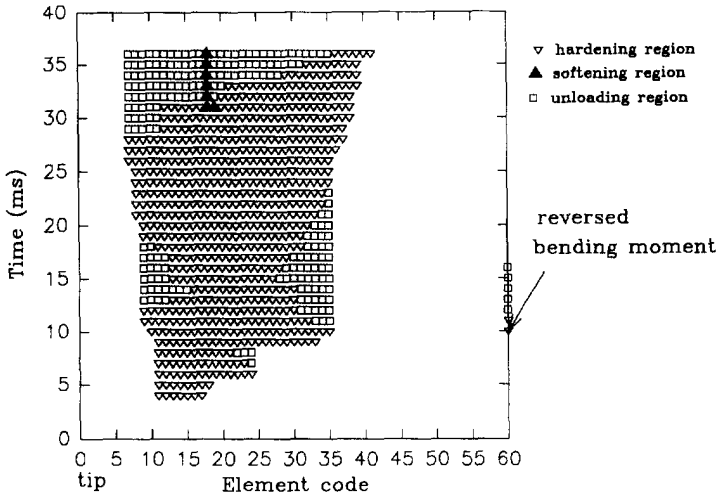

Fig. 12. The evolution of plastic regions for Example 2.

at one end, so that the elastic flexural waves reflected at the clamped end greatly influence the distribution of bending moment. When the maximum curvature reaches the critical value κ_{cr}, the bending moment distribution has reached a steady state. Consequently, the softening region concentrates at the cross-section where the bending moment is a maximum.

In order to reveal whether or not the softening region can grow, two other constitutive models are selected in this section in which the critical curvature κ_{cr} is set much smaller than 1.54 m^{-1} in order to initiate the softening phase before a steady state of moment distribution has been attained.

The loading constitutive equations for the two models are:
Model A

$$M = \begin{cases} EI\kappa, & \kappa < \kappa_e \\ 1050 + 1530(\kappa - \kappa_e), & \kappa_e < \kappa < \kappa_{cr} \\ 1755[1 - \alpha(\kappa - \kappa_{cr})], & \kappa_{cr} < \kappa, \end{cases}$$

with $\kappa_{cr} = 0.5\ m^{-1}$, $\kappa_e = 0.03924\ m^{-1}$, $\alpha = 0.01$;
Model B

$$M = \begin{cases} EI\kappa, & \kappa < \kappa_e \\ 1050 + 733.8(\kappa - \kappa_e), & \kappa_e < \kappa < \kappa_{cr} \\ 1755[1 - \alpha(\kappa - \kappa_{cr})], & \kappa_{cr} < \kappa, \end{cases}$$

with $\kappa_{cr} = 1.0\ m^{-1}$, $\kappa_e = 0.03924\ m^{-1}$, $\alpha = 0.01$.

The external force applied at the tip is a linearly decaying pulse with a mean magnitude identical to that in the previous two examples. It is expressed by

$$P(t) = 16.884 - 482.400t,$$

with P in kilonewtons (kN) and t in seconds (s).

The positions of the softening regions in the tubular beam during the response of the two models are as shown in Figs. 13(a) and 13(b), respectively. Unlike the first example described in Section 3.1, the softening region extends towards the root after the softening phase is initiated at one cross-section. The length of the softening region reaches 0.4 m ($\approx 0.13L$) as shown in Fig. 13. The time interval from the initiation of softening to final localization, at which the expanded softening region shrinks to a single cross-section, is approximately 5.6 ms for Model A and 10 ms for Model B.

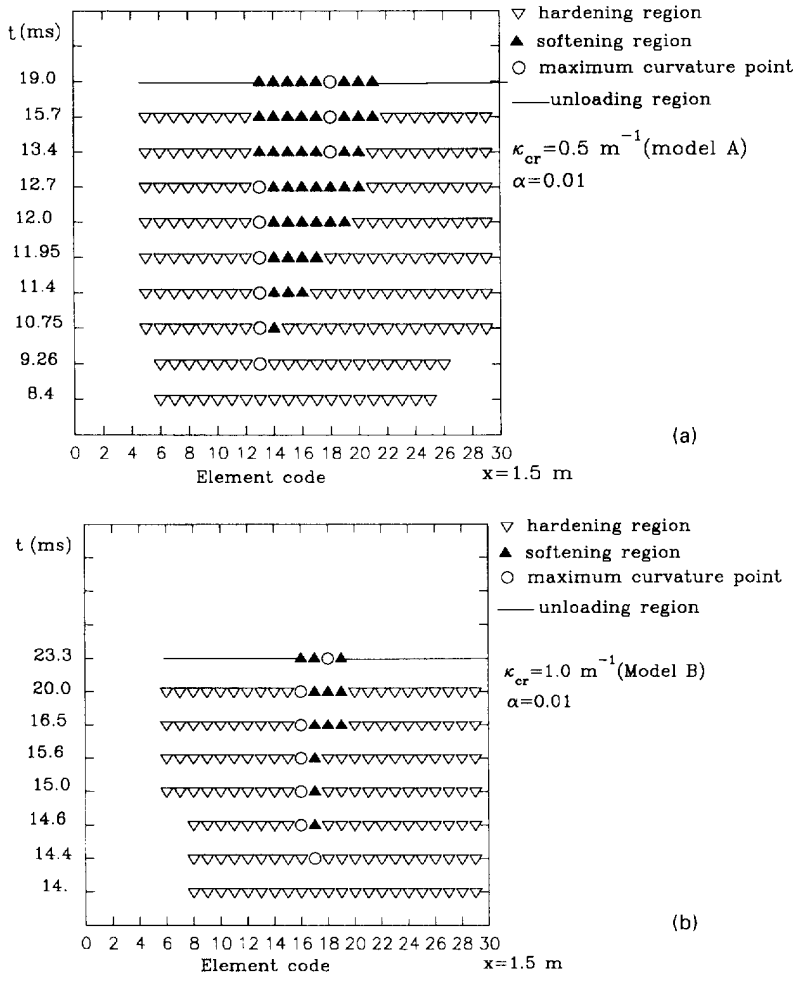

Fig. 13. (a) Evolution of plastic regions for Example 3, model A; (b) evolution of plastic regions for Example 3, model B.

The cross-section with maximum curvature in the softening region is not always restricted to the initial softening section but possibly changes its position. This is confirmed by Fig. 13. Therefore, which section becomes the final localized softening position depends upon whether or not its curvature is the maximum of those for all of the softening sections when unloading occurs in the beam.

4. CONCLUDING REMARKS

The elastic–plastic dynamic response of a tubular cantilever beam which possesses hardening and softening characteristics has been studied by a numerical procedure based on a small deflection formulation. The effects of strain-hardening of the material and the ovalization of tubular cross-sections have been incorporated into a plastic hardening/softening relation between the bending moment and the centre line curvature. The rotary inertia of beams elements has also been included so as to attain a better simulation of the propagation of elastic flexural waves.

Numerical examples demonstrate that this finite difference procedure provides predictions of distributions of bending moment and plastic curvature in excellent agreement with those obtained from finite element analysis (Reid and Gui, 1987). Another example which utilizes parameters selected from a pipe-whip test (Wang, 1991) when compared with experiment data gives good predictions for the region influenced by ovalization and for the deflected shape of the pipe. All of these verify that the theoretical model and the numerical

procedure are appropriate for analysing the dynamic behaviour of flexible tubular beams subjected to intense pulse/impulsive loading.

One notable feature observed from the numerical results is that softening may be confined to a single cross-section, or it may extend over a region of finite length away from the loading point. As indicated by the third example, whether the softening region extends or not depends on the magnitude and the shape of the loading pulse, as well as on the detailed character of the hardening/softening M-κ curve. This conclusion is contrary to that for the static case, for which Wood (1968) showed that softening cannot occur in a region of finite length. This is because in the dynamic case the inertia of the beam results in bending moment diagrams continually changing with time. This allows the bending moment generated at some cross-sections to increase and reduce, resulting in hardening and softening. On the other hand, the development of a softening region in a finite beam is restricted, unlike that in a semi-infinite beam (Yu and Li, 1993; Wang *et al.* 1994) in which the softening region can continuously extend with increase of time. The limited length of the softening region in finite beams is attributed to the unloading in the plastic region caused by the reflected elastic flexural waves, as explored by Reid and Gui (1987) as well as by the numerical examples in the present paper.

The numerical results obtained in the present study are also substantially different from those given previously by Stronge and Yu (1989). By adopting a rigid-hardening (or softening) $M \sim \kappa$ relation and neglecting the inertia of the plastically deforming segment close to the root, Stronge and Yu (1989) found that for a rigid-hardening (or softening) cantilever beam subjected to impact loading at the tip, the final curvature increases from the tip towards the root. The present model provides an entirely different picture of the location of the softening region and the final distribution of plastic curvature. This is because in the present model we have correctly incorporated the effects of elasticity and inertia in the entire beam. As pointed out by Yu (1993) and by Reid and Gui (1987), in comparison with rigid-plastic analyses, taking elasticity into account dramatically alters the shape of the bending moment diagram for a cantilever beam subjected to impact, so that the peak moment appears at an inner cross-section, where softening may be initiated, instead of at the root.

The major limitation of the present model is the assumption of small deflections. This will be removed in a future study, so that the effects of geometry change and axial forces can be investigated. Furthermore, the possible formation of a localized buckle (kink) in the tubular beam will be of particular interest.

Acknowledgements—The work described was conducted as part of a research contract funded by a grant from the Engineering and Physical Science Research Council (EPSRC) under grant number, GR/H82174. The authors would like to express their gratitude for this support.

REFERENCES

Brazier, L. G. (1926). On the flexure of thin cylindrical shells and other sections. *Proc. R. Soc. Series A* **CXVI,** 104–114.

Calladine, C. R. (1982). Plastic buckling of tubes in pure bending. In *Collapse: the Buckling of Structures in Theory and Practice: IUTAM Symposium*, pp. 111–124. Cambridge University Press, Cambridge, U.K.

Jones, N. and Wierzbicki, T. (1987). Dynamic plastic failure of a free-free beam. *Int. J. Impact Engng* **6,** 225–240.

Kyriakides, S. and Ju, G. T. (1992). Bifurcation and localisation instabilities in cylindrical shells under bending—I. Experiments. *Int. J. Solids Structures* **29,** 1117–1142.

Martin, J. B. (1989). Dynamic bending collapse of strain-softening cantilever beams. *Structural Failure* (Edited by T. Wierzbicki and N. Jones), pp. 369–388. Wiley, New York.

Reddy, B. D. (1979). An experimental study of the plastic buckling of circular cylinders in pure bending. *Int. J. Solids Structures* **15,** 669–676.

Reid, S. R. and Gui, X. G. (1987). On the elastic-plastic deformation of cantilever beams subjected to tip impact. *Int. J. Impact Engng* **6,** 109–127.

Reid, S. R. and Prinja, N. K. (1989). The mechanics of pipe whip. *Proc. Conf. on Pipework Engng and Operation*, I. Mech. E., Paper C376/044, 315–326, Feb. 1989.

Reid, S. R., Yu, T. X. and Wang, B. (1992). Analytical modeling of pipe whip. Final Report, Nuclear Electric Contract-CON/BC 2273.

Stronge, W. J. and Yu, T. X. (1989). Dynamic plastic deformation in strain-hardening and strain-softening cantilevers. *Int. J. Solids Structures*, **25,** 769–782.

Symonds, P. S. and Fleming, W. T. (1984). Parkes revisited : on rigid-plastic and elastic-plastic dynamic structural analysis. *Int. J. Impact Engng* **2,** 1–36.
Wang, B. (1991). Response of two-dimensional piping systems during pipe whip. PhD Thesis, UMIST.
Wang, X. D., Yu, T. X. and Meguid, S. A. (1994). On the dynamic analysis of an ideally-plastic sofening beam. *Int. J. Impact Engng* **15,** 279–309.
Wood, R. H. (1968). Some controversial and curious developments in the plastic theory of structures. In *Engineering Plasticity* (Edited by J. Heyman and F. A. Leckie), pp. 665–691. Cambridge University Press, Cambridge, U.K.
Yu, T. X. (1993). Elastic effects in the dynamic plastic response of structures. In *Structural Crashworthiness and Failure* (Edited by N. Jones and T. Wierzbicki), Ch. 9. Elsevier, Amsterdam.
Yu, T. X. and Li, H. L. (1993). Dynamic response of a semi-infinite elastic-softening beam to impact, Proc. 1st Asia–Oceania Int. Symp. on Plasticity, 16–19 August 1993, Beijing, China.
Yu, T. X., Reid, S. R. and Wang, B. (1993). Hardening-softening behaviour of tubular cantilever beams. *Int. J. Mech. Sci.* **35,** 1021–1033.

APPENDIX

In order to examine the effectiveness of the computer program used in the present study of the dynamic plastic behaviour of tubular beams with global hardening–softening properties, this appendix reproduces some results obtained by Reid and Gui (1987) who used the finite element code ABAQUS. All of the parameters selected here for the sample problem [Example 1 in Reid and Gui (1987)] are the same as those in Reid and Gui (1987) (see Table A). It should be noted that the formulation presented in this study is based on small deflection theory and ignores the transverse shear effect, which was taken into account in Reid and Gui's paper but was limited to elastic deformation only.

Figs A1–A4 give the distributions of bending moment over the time interval from $t = 0.065$ ms to $t = 3.590$ ms. The curves are very close to Fig. 3(a,b,c,d) in Reid and Gui's paper and verify that the key features resulting from the inclusion of elasticity in the finite element approach are retained by the present numerical procedure.

Table A

Parameters	Example 1 $R = 14.8$	Parameters	Example 1 $R = 14.8$
E (N mm^{-2})	2.069×10^5	G (kg)	0.336
σ_0 (N mm^{-2})	200	V_0 (m s^{-1})	12.9
M_0 (Nm)	16.5	$\beta = \rho Lbh/2G$	0.305
ρ (kg m^{-3})	7850	K_0 (J)	27.9
L (mm)	355.6	$R = 2K_0EI/M_0^2L$	14.8
b (mm)	16.3	No. of elements	28
h (mm)	4.5		

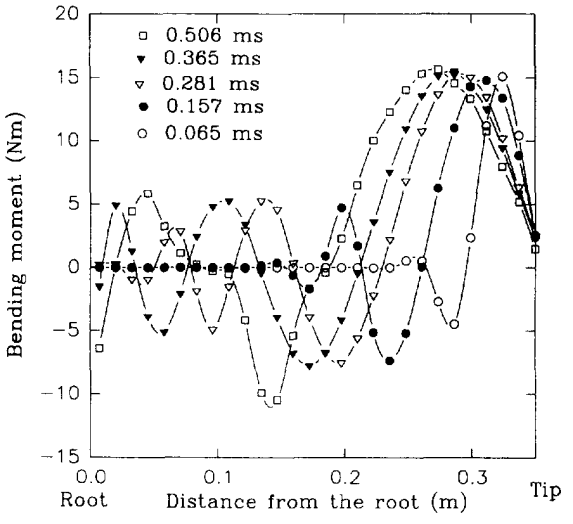

Fig. A1. Bending moment diagram at various instants, showing flexural wave motion (from 0.065 to 0.506 ms).

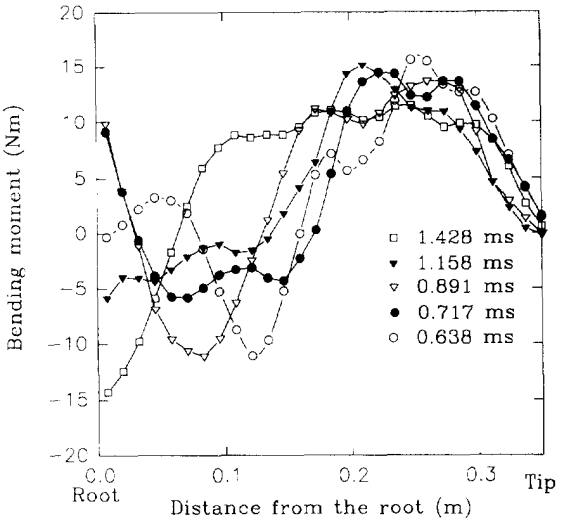

Fig. A2. Bending moment diagram at various instants, showing flexural wave motion (from 0.638 to 1.428 ms).

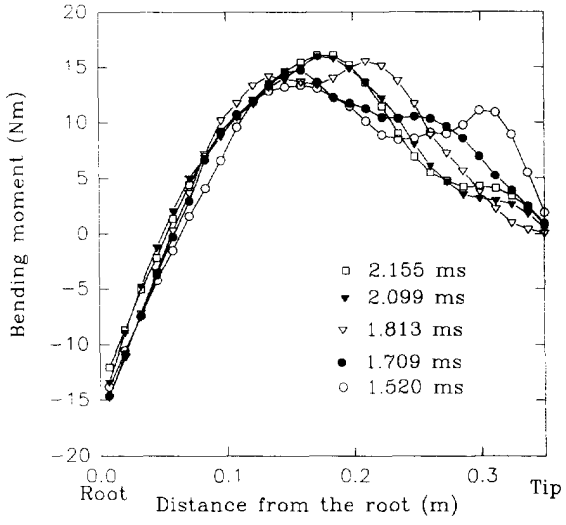

Fig. A3. Bending moment diagram at various instants, showing flexural wave motion (from 1.520 to 2.155 ms).

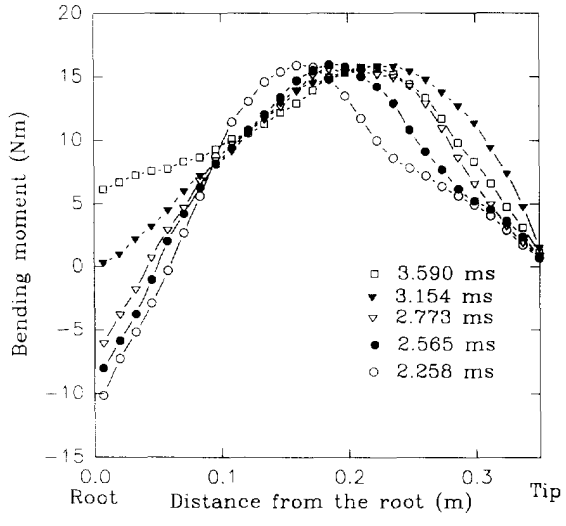

Fig. A4. Bending moment diagram at various instants, showing flexural wave motion (from 2.258 to 3.590 ms).